Reaction of the 4-Biphenylnitrenium Ion with 4-Biphenyl Azide to Produce a 4,4′-Azobisbiphenyl Stable Product: A Time-Resolved Resonance Raman and Density Functional Theory Study

Jiadan Xue, Yong Du, Xiangguo Guan, Zhen Guo, and David Lee Phillips*

Department of Chemistry, The University of Hong Kong, Pokfulam Road, Hong Kong, P. R. China

Received: June 18, 2008; Revised Manuscript Received: September 16, 2008

A time-resolved resonance Raman (TR^3) and density functional theory (DFT) study of the reaction of the 4-biphenylnitrenium ion with 4-biphenyl azide in a mixed aqueous solution is reported. The reaction of the 4-biphenylnitrenium ion with its unphotolyzed precursor 4-biphenyl azide in a mixed aqueous solution generates a 4,4′-azobisbiphenyl stable product via an intermediate species. With the aid of DFT calculations for likely transient species, this intermediate was tentatively assigned to a 4,4′-azobisbiphenyl cation. The DFT calculations predict this reaction can take place via two pathways that compete with one another to produce the *trans* and *cis* 4,4′-azobisbiphenyl product. The observation of the 4,4′-azobisbiphenyl cation intermediate demonstrates that the reaction of the arylnitrenium ion with its aryl azide to produce a stable azo product occurs via a stepwise mechanism.

Introduction

Arylnitrenium ions are key reaction intermediates in the carcinogenic reaction of aromatic amines with DNA guanine, and there is much interest in studying their properties and reaction with other species.[1−15] The 4-biphenylnitrenium and 2-fluorenylnitrenium ions have been of particular interest because their corresponding arylamines were found to be a component of cigarette smoke and diesel exhaust.[35] In addition, these two nitrenium ions are able to be generated with excellent yields by photolysis of aryl azides in an aqueous solution (see Scheme 1),[18−20] and this enables time-resolved spectroscopic measurements to be applied to study the detailed properties of arylnitrenium ions.[11,15−19] Transient absorption experiments determined that the 2-fluorenylnitrenium ion reacts with water and guanosine with rate constants of 3×10^4 s^{-1} and 7.6×10^8 M^{-1} s^{-1}, respectively.[13,35] The 4-biphenylnitrenium ion was found to be more reactive toward water, and a rate constant of about 2×10^6 s^{-1} was determined.[13,35] Time-resolved resonance Raman (TR^3) experiments have been used to characterize 4-biphenylnitrenium and 2-fluorenylnitrenium ions in mixed water solvents and found that the 2-fluorenylnitrenium ion has a significantly stronger iminocyclohexadienyl character compared to the 4-biphenylnitrenium ion due to the 2-fluorenylnitrenium ion having a more planar structure between the two phenyl rings and increased charge delocalization into the phenyl rings.[21,22] Picosecond and nanosecond TR^3 experiments have directly shown that the 2-fluorenylnitrenium ion is generated about 100 ps after photolysis of 2-fluorenyl azide in a mixed aqueous solvent[23] and that the 2-fluorenylnitrenium ion reactions with several guanine derivatives to produce C8 intermediates were also observed.[24]

In the case of the 4-biphenylnitrenium ion, a number of studies have been performed by using a variety of techniques, including transient absorption, transient Raman, and IR combined with argon/HCl matrices characterization of the 4-biphenylnitrenium ion,[18,22,26] the product analyses showing that 4-hydroxy-4-phenyl-2,5-cyclohexadienone is one of the major products after photolysis of 4-biphenyl azide in a mixed aqueous solution.[27] However, there are few studies on the reactivity of the 4-biphenylnitrenium ion with other species on the nanosecond−microsecond time scales or direct time-resolved vibrational spectroscopic observation of the reaction of the 4-biphenylnitrenium ion with other species. In this paper, 4-biphenyl azide was employed as a precursor to generate the 4-biphenylnitrenium ion in a mixed aqueous solution. The TR^3 experimental results on the nanosecond−microsecond time scales showed that the reaction of the 4-biphenylnitrenium ion with 4-biphenyl azide first produces an intermediate that then further decays to form a stable azo compound product, 4,4′-azobisbiphenyl. This sequence of events appears different from our previous observation that the 2-fluorenylnitrenium ion reacts with its unphotolyzed precursor 2-fluorenyl azide in a mixed aqueous solution to form a corresponding azo compound.[25] The direct observation of the intermediate leading to the azo compound here clearly demonstrates that the reaction of the 4-biphenylnitrenium ion with 4-biphenyl azide takes place in a stepwise manner rather than in a concerted manner. DFT calculations were used to predict structures and Raman spectra of likely intermediate

SCHEME 1: Three Competing Pathways after Photolysis of an Aryl Azide in an Aqueous Solution: (1) Intersystem Crossing (ISC) to Form a Triplet Nitrene Species; (2) Ring Expansion to Form a Didehydroazepine (Cyclic Ketenimine) Species through an Azirine Intermediate; (3) Protonation to Produce an Arylnitrenium Ion Species

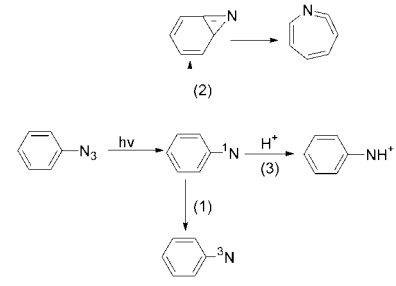

* Author to whom correspondence should be addressed. Telephone: 852-2859-2160. Fax: 852-2857-1586. E-mail: phillips@hkucc.hku.hk.

10.1021/jp805353q CCC: $40.75
Published on Web 10/29/2008

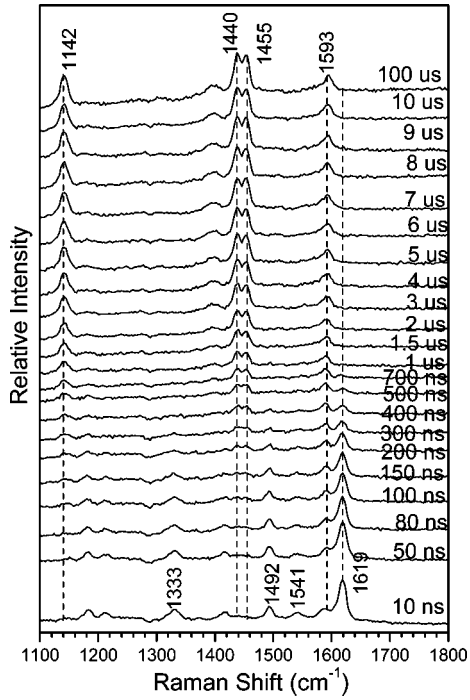

Figure 1. Overview of 354.7 nm probe wavelength TR^3 spectra obtained after 299.1 nm photolysis of 1 mM 4-biphenyl azide in a water: acetonitrile(60:40 by volume) mixed solvent.

species in order to help assign the observed species. The DFT computational results suggest that the reaction of the 4-biphenylnitrenium ion with 4-biphenyl azide can proceed via two competing pathways to produce *trans* and *cis* 4,4′-azobisbiphenyl.

Results and Discussion

Results of Nanosecond Time-Resolved Resonance Raman (TR^3) Experiments. Figure 1 and Figure 1S in the Supporting Information display TR^3 spectra acquired at various time delays after photolysis of 1 mM (Figure 1) and 2 mM (Figure 1S in the Supporting Information) 4-biphenyl azide in a water: acetonitrile (60:40 by volume) mixed solvent. The time delays between the pump (299.1 nm) and the probe (354.7 nm) laser beams are shown to the right of each spectrum, and the Raman shifts of selected bands are presented at the top of 100 μs and 10 ns spectra in these figures. The TR^3 spectra shown in Figures 1 and 1S are similar to one another and indicate that three species can be observed over a range from 10 ns to 100 μs. The first species has characteristic Raman bands at 1619, 1541, 1492, and 1333 cm^{-1} and appears to decay within several hundred nanoseconds and to be a precursor of the other two species. This first species was observed before and characterized as the 4-biphenylnitrenium ion.[22] Details are provided in Figure 2s in the Supporting Information. The second species has a characteristic Raman band at 1590 cm^{-1} (this overlaps somewhat with bands of the other two species) and appears to first grow in and then decay. The third species has characteristic bands at 1593, 1455, 1440, and 1142 cm^{-1} and appears to grow in and does not decay over the several hundred microseconds time scale. Oxygen purged TR^3 experiments have also been performed, and these results showed that all three species are not sensitive to oxygen.

The third species has two prominent resonance Raman bands in the 1400−1500 cm^{-1} region characteristic of N=N bond stretching vibrational modes and was identified to be 4,4′-azobisbiphenyl from comparison of the TR^3 spectra to DFT calculated Raman spectra of 4,4′-azobisbiphenyl species and a resonance Raman spectrum obtained for an authentic sample of 4,4′-azobisbiphenyl made by another synthetic method (see Figure 3S and description of the assignment in the Supporting Information). Here, we cannot exclude the possibility that *cis* 4,4′-azobisbiphenyl was generated, because *cis* and *trans* 4.4′-

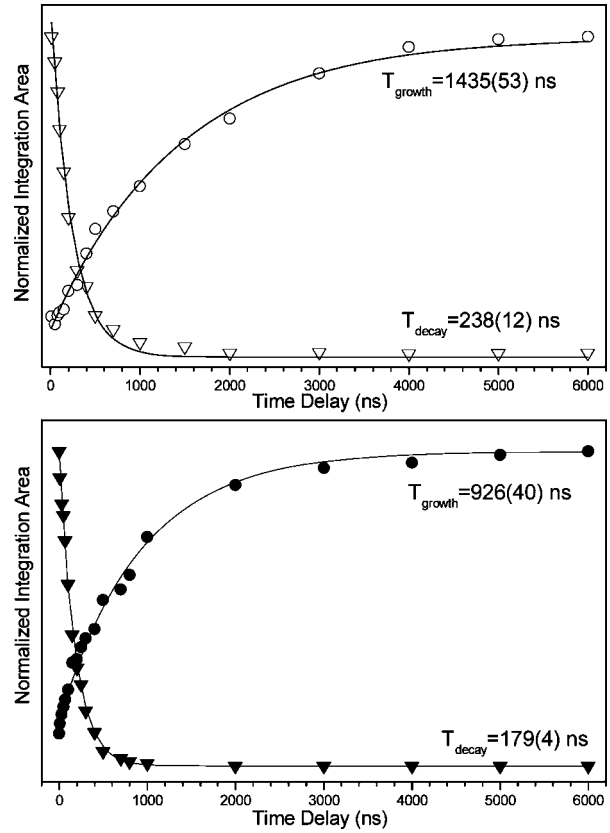

Figure 2. Plots of the integrated areas for the characteristic Raman bands for the 4-biphenylnitrenium ion (1619 cm^{-1}) and the 4,4′-azobisbiphenyl (1440 cm^{-1}) species observed in the TR^3 spectra of Figure 1 and Figure 1S in the Supporting Information as a function of time delay are shown. Top: from Figure 1, 1 mM of precursor used; open circles, 4,4′-azobisbiphenyl; open triangles, 4-biphenylnitrenium ion. Bottom: from Figure 1S, 2 mM of precursor used; closed circles, 4,4′-azobisbiphenyl; closed triangles, 4-biphenylnitrenium ion. The time constants for the best fit exponential kinetics are indicated next to the appropriate curves. The bracketed numbers are fitted uncertainties.

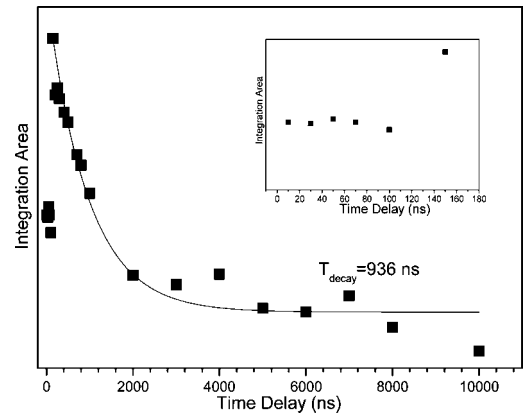

Figure 3. Plots of the integrated areas for the 1593 cm^{-1} Raman band observed in the TR^3 spectra of Figure 1S in the Supporting Information as a function of time delay are shown. These integration areas have been subtracted for the contribution of the 4,4′-azobisbiphenyl species. The insert displays the data obtained at early time delays.

SCHEME 2

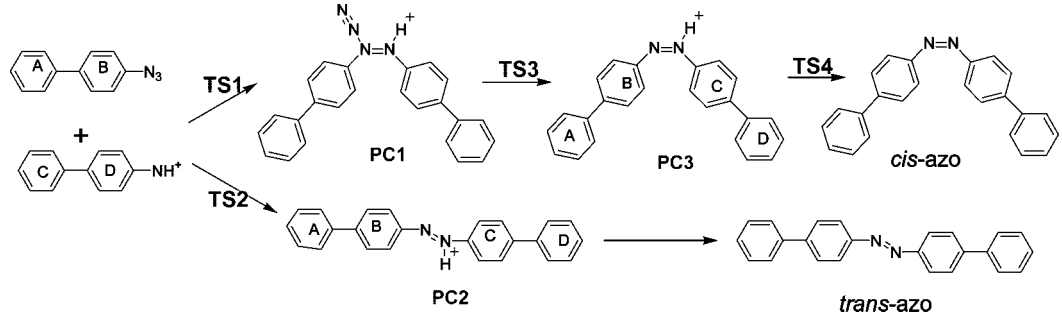

TABLE 1: Comparison of Distance of Selected Atoms in Reactants, Transition States, and Intermediates and Dihedral Angles Related to Nitrogen Atoms Shown in Figure 4

	R_{12} (Å)	R_{23} (Å)	R_{57} (Å)	R_{24} (Å)	R_{45} (Å)	R_{46} (Å)	D_{1246} (deg)
RC1	1.4049	1.2526		2.5674	1.0266	1.3083	−18.46
TS1	1.4452	1.2718		1.6229	1.0221	1.4086	26.84
PC1	1.4522	1.2810		1.4613	1.0199	1.4388	51.22
TS3	1.4546	1.3114		1.3608	1.0133	1.4270	65.87
PC3a	1.3663	4.7635		1.2826	1.0222	1.4250	15.36
PC3b	1.4022		2.0671	1.3075	1.0162	1.4790	49.08
TS4	1.4032		1.9087	1.2851	1.0241	1.4515	39.79
PC4	1.4294		0.9788	1.2529	2.0321	1.4321	11.03
RC2	1.4098	1.2379		2.8382	1.0275	1.3041	42.98
TS2	1.4310	1.2788		1.7401	1.0258	1.3722	7.75
PC2	1.3675	3.9379		1.2793	1.0253	1.4002	0.23

TABLE 2: Calculated Barrier and Reaction Energies at B3LYP/6-31g* with ZPE Corrections (unit: kcal/mol)

	gas phase		aqueous phase	
	barrier	reaction energies	barrier	reaction energies
cis pathway **(TS1)**	13.87	13.02	6.83	−5.53
cis pathway **(TS3)**	3.06	−80.34	−1.96	−65.06
cis pathway **(TS4)**	0.19	−45.90	4.16	−42.38
trans pathway **(TS2)**	12.70	−76.30	7.30	−80.50

azobisbiphenyl isomers exhibit spectrally well-separated absorption bands in the UV−visible absorption spectrum[32] as shown in Figure 4S in the Supporting Information. The absorption spectrum of the synthesized 4,4′-azobisbiphenyl displays low-lying (nπ*) bands between 420 and 600 nm and the π π* bands at 360 nm (*trans*) and 250 nm (*cis*). The 355 nm probe laser used in the TR^3 experiment makes the *trans* azo isomer resonantly enhanced; therefore, for both the synthesized 4,4′-azobisbipheny and the transient species generated during TR^3 experiment, mainly the *trans* isomer was observed when using the conditions employed in the TR^3 experiments. Because the characteristic absorption band of the *cis* azo form (λ_{max} 250 nm) overlaps somewhat with that of 4-biphenyl azide, it is difficult to select an appropriate probe wavelength to selectively resonantly enhance the *cis* azo isomer by itself in the TR^3 experiment.

Precursor of the 4,4′-Azobisbiphenyl Product: Time-Dependent Behavior of Species Observed in the TR^3 Spectra. To examine the kinetic behavior of the three species observed in the TR^3 spectra of Figure 1 and Figure 1S in the Supporting Information, the characteristic Raman bands for the 4-biphenylnitrenium ion at 1619 cm^{-1} and for the 4,4′-azobisbiphenyl product at 1440 cm^{-1} had their integrated areas plotted as a function of time delay in Figure 2. Each of the four kinetics curves in Figure 2 was normalized to the largest Raman band intensity observed for each species over the 10 ns to 100 μs TR^3 spectra shown in Figure 1 and Figure 1S in the Supporting Information, respectively. The kinetics of the 4-biphenylnitrenium ion decay can be fitted satisfactorily to a single-exponential decay function with time constants of approximately 238 ns in a 1 mM concentration solution and 179 ns in a 2 mM concentration solution. The kinetics of the 4,4′-azobisbiphenyl growth can be fitted to a single-exponential growth function with time constants of approximately 1435 ns in a 1 mM concentration solution and 926 ns in a 2 mM concentration solution. These concentration dependences indicate that the 4-biphenylnitrenium ion is quenched by 4-biphenyl azide. The decay time ratios of the 4-biphenylnitrenium ion (238 ns:179 ns) in the two different concentration solutions is not as big as that of the third species growth (1435 ns:926 ns) in the two different concentration solutions. This may be due to the low signal-to-noise of the spectra perturbing the time constant fitting for the 4-biphenylnitrenium ion. Figure 3 displays the integrated areas for the 1593 cm^{-1} Raman band observed in the TR^3 spectra in Figure 1S in the Supporting Information plotted as a function of time delay. These integration areas in Figure 3 have been subtracted for the contribution of the third species, 4,4′-azobisbiphenyl. Inspection of Figure 3 shows that the data after 150 ns (including 150 ns) time delay can be fitted well by a single exponential decay function with a time constant of 936 ns. This is in agreement with the 926 ns growth time constant of the third species. As shown in the inset of Figure 3, the data before 150 ns time delay stays about the same, in which the total contributions come from both the 4-biphenylnitrenium ion decrease and the intermediate increase. These results combined with the dependence of the 4-biphenylnitrenium ion decay and the 4,4′-azobisbiphenyl growth on the azide concentration strongly suggest that the 4-biphenylnitrenium ion reacts with 4-biphenyl azide to generate the intermediate that subsequently produces the 4,4′-azobisbiphenyl product. The triplet 4-biphenylnitrene was directly observed before in neat acetonitrile to produce 4,4′-azobisbiphenyl.[29] Here, the triplet 4-biphenylnitrene was eliminated because its spectrum does not match that of the intermediate (see Figure 5S in the Supporting Information), which also demonstrates that, at the conditions used here in the TR^3 experiments, the 4-biphenylnitrenium ion will not convert to its conjugate base, the singlet nitrene that can then generate a triplet nitrene by intersystem crossing (ISC).

Possible Assignments for the Intermediate: DFT Results for Some Likely Species. The direct observation of the intermediate in the TR^3 experiments indicates that the reaction of the 4-bipenylnitrenium ion with 4-biphenyl azide to produce the 4,4′-azobisbiphenyl product takes place in a stepwise manner. Therefore, DFT calculations were performed to help assign the observed intermediate and to study the details of the reaction mechanism. Two competing reaction pathways were found, and these are shown in Scheme 2. In one pathway, the

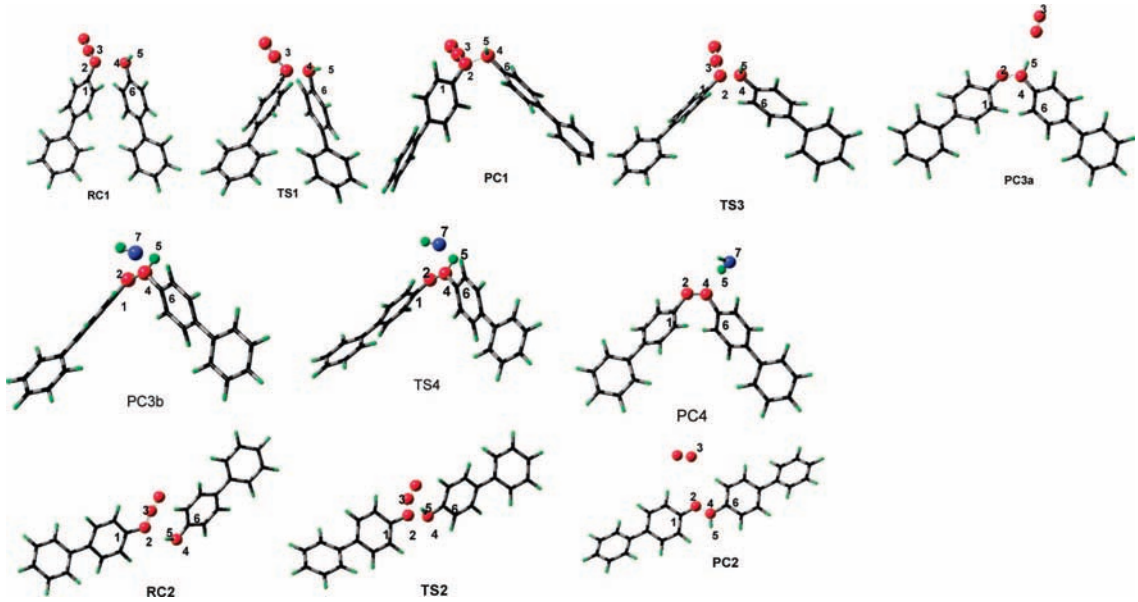

Figure 4. Optimized geometries are shown for the reactant complexes, transition states, and intermediates.

reaction of the 4-biphenylnitrenium ion with 4-biphenyl azide loses N_2 and H^+ sequentially to give rise to **PC**1 and **PC3** as two intermediates and then generates *cis*-azobisbiphenyl (referred to as the *cis* pathway hereafter). In the other pathway, this reaction loses N_2 directly to produce **PC2** as an intermediate and subsequently produces the stable *trans*-azobisbiphenyl (referred to as the *trans* pathway hereafter). The optimized geometries for all of the reactant complexes (RC, azide, and nitrenium ion complex), transition states (TS), and intermediates (PC) obtained from the B3LYP/6-31g* calculations are presented in Figure 4. Table 1 shows the distances of selected atoms and the dihedral angle around the nitrogen atoms. Examination of Figure 4 and Table 1 show that, in both the *cis* and the *trans* pathways, as the reaction goes from **RC**1 (**RC2**) to **PC3a (PC2)**, the distances of N2−N4 always decrease and those of N2−N3 always increase. These results are consistent with the process that a new bond forms between the N2 and N3 atoms and then loses N_2 to generate an azo cation species (**PC2** and **PC3**).

With the help of a hydroxide ion (this may come from the protonation process of forming the nitrenium ion), the azo cation can lose H^+ to produce a neutral azo species. In the *cis* pathway, a transition state (**TS**4) was located. Examination of Figure 4 and Table 1 shows that in the presence of a hydroxide ion, the bond lengths of N2−N4, N4−H6, and H6−O7 all decrease while the reaction goes from the azo cation (**PC3b**) through **TS4** to make the *cis* 4,4′-azobisbiphenyl species. This appears to correspond to a process in which the H^+ leaves the azo cation to produce a water molecule from reaction with a hydroxide ion, and the N−N single bond turns into a N═N double bond. The dihedral angle of C1−N2−N4-C6 changes distinctly during the reaction process, from 49°(**PC3b**) to 40°(**TS4**) to 11°(*cis* 4,4′-azobisbiphenyl). This obvious change of the C1−N2−N4−C6 dihedral angle reveals that the dihedral angle twist also serves as a driving force for the H^+ to leave the azo cation. There is some change in the geometry of the azo cation in the presence of a hydroxide ion as shown in Figure 4 and Table 1. The bonds of C1−N2, N2−N4, and N4−C6 are all elongated because of the presence of the hydroxide ion. The dihedral angles of C1−N2−N4−C6 are different without and with the presence of a hydroxide ion, and they are 15.4° and 49.1°, respectively. This kind of change in the geometries of the azo cation species is reasonable to take place as a result of the stabilization of the hydroxide ion.

In the *trans* pathway, the dihedral of C1−N2−N4−C6 angles are almost 0° in both **PC2** and *trans* 4,4′-azobisbiphenyl; therefore, the lack of the aid of a dihedral angle twist increases the demand of the attraction from the hydroxide ions. The TR[3] experiments were performed in an aqueous solution, in which hydroxide ions and water molecules exist around the reactants and interact with the reactant molecules and with each other. This situation is very difficult to actually mimic with the simple calculations done here, and hence, no reasonable transition states were found to connect **PC**2 and *trans* 4,4′-azobisbiphenyl from the DFT calculations although this reaction is likely to occur under experimental conditions.

The reaction of the 4-biphenylnitrenium ion with 4-biphenyl azide occurs in an aqueous solution; therefore, the solvent effect on the reaction was examined. Table 2 lists the calculation results for the activation barrier and reaction energies in the gas and aqueous phases. Compared with the data obtained in the gas phase, the solvent effect decreases the barrier and reaction energies substantially, especially for the steps through **TS1** and **TS2**. Examination of Table 2 shows that all of the reactions are exothermic in the aqueous phase, which implies that the reaction of the 4-biphenylnitrenium ion with 4-biphenyl azide to form 4,4′-azobisbiphenyl is more likely to occur in an aqueous solution. Figure 5 presents the relative energy profile in the aqueous phase and shows that there is no distinct difference between the activation barriers for the first step of the *cis* and *trans* pathways (6.8 and 7.3 kcal/mol respectively). Therefore, within the calculation error, the *cis* and *trans* pathways should be parallel and competing with each other, even though the reaction mechanisms on the two pathways are different. On the *cis* pathway, the reaction mechanism shown in Figure 5 shows that a new N−N bond formation between the azide and the nitrenium ion occurs; then, the leaving of the N_2 and H^+ species takes place in a stepwise manner to produce two intermediates, **PC1** and **PC3**, respectively. **PC1** is not stable, and it is easy for elimination of N_2 to occur and produce the azo cation (**PC3**) with only a small barrier in the aqueous solution. The **PC3** species with the aid of a hydroxide ion and the driving force of the dihedral angle changes can lose the H^+

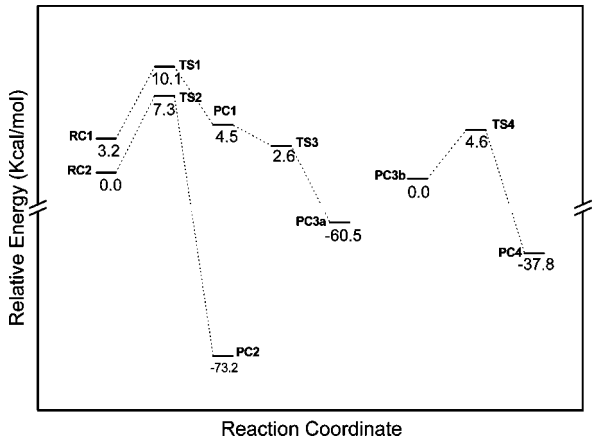

Figure 5. Relative energy profiles (in kcal/mol) obtained from the B3LYP/6-31g* calculations. The values of **PC3b**, **TS4**, and **PC4** were obtained relative to **PC3b**, and the others were obtained relative to **RC2**.

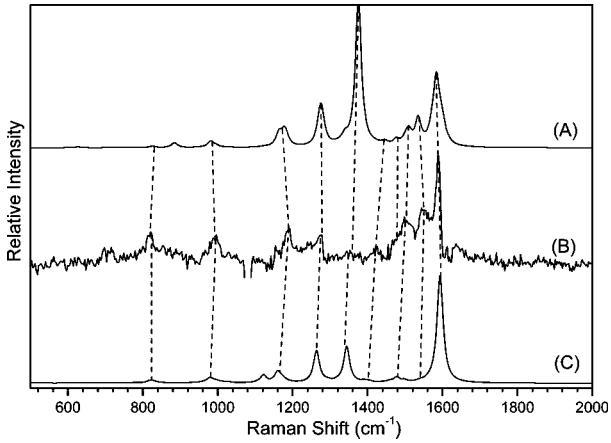

Figure 6. Comparison of the B3LYP/6-31g* calculated normal Raman spectra of azo cation (A) *trans* (**PC2**) and (C) *cis* (**PC3b**) isomers to (B) the experimental TR^3 spectrum of the intermediate.

group and finally generate the *cis* 4,4′-azobisbiphenyl species. In contrast, on the *trans* pathway, the N−N bond formation between the azide and nitrenium ion and the N_2 group leaving take place simultaneously and therefore produce only one intermediate, **PC2**. With the presence of hydroxide ions and water molecules, this **PC2** could lose H^+ to produce the *trans* 4,4′-azobisbiphenyl, although no reasonable transition states were found from DFT calculations because of our limited model compared to the complexity of this process.

Because the first step of the *cis* and *trans* pathways are similar to one other and both likely to occur, the *cis* and *trans* isomers of the azo cation and 4,4′-azobisbiphenyl species could both be produced in the TR^3 experiments (the reasons that only *trans* 4,4′-azobisbiphenyls was observed when using the TR^3 conditions used here have already been presented in an early section). Inspection of the relative energy profiles (Figure 5) shows that the **PC3b** species is a relative stable intermediate (it is like a *cis* azo cation with a hydroxide ion around it). Similarly, the *trans* azo cation (**PC2**) could also be a stable intermediate, because no change in the geometry can be observed when one hydroxide ion was put around *trans* azo cation. Therefore, the possibility that the intermediate observed in TR^3 spectra is species **PC2** and **PC3b** was examined here, as shown in Figure 6. Examination of Figure 6 reveals that the experimental spectrum shows reasonable agreement with the calculated spectrum for the *trans* and *cis* azo cations with some moderate

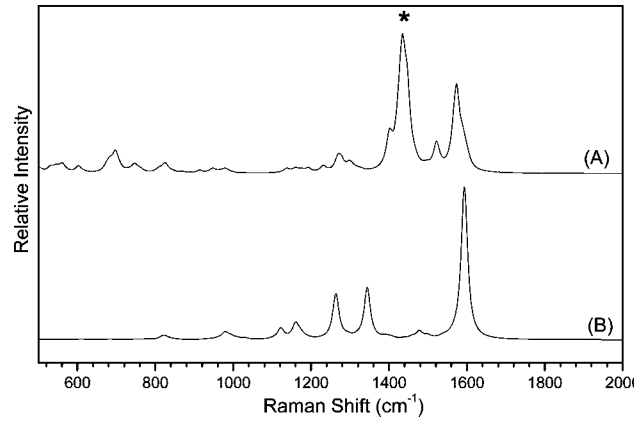

Figure 7. Comparison of the B3LYP/6-31g* calculated normal Raman spectra of the *cis* azo cation (A) **PC3a** without a hydroxide ion nearby to (B) **PC3b** with a hydroxide ion near the cation. The star indicates the Raman band associated with the N═N stretching mode.

differences in the relative intensities that can be easily accounted for by noting that the experimental spectra are resonantly enhanced whereas the calculated spectra are for normal (or nonresonant) Raman spectra. Tables 1S and 2S in the Supporting Information show that there is generally good agreement between the experimental and calculated vibrational frequencies, the calculated vibrational frequencies being within about 5 and 7 cm^{-1} on average for the 13 experimental Raman band frequencies for the *trans* and *cis* azo cation, respectively, compared to calculated ones. These results suggest that the ns-TR^3 spectra in Figures 1 and 1S in the Supporting Information for the intermediate observed from the reactions of the 4-biphenylnitrenium ion with 4-biphenyl azide can be tentatively assigned to the *trans* and *cis* azo cation.

In Table 1S in the Supporting Information, there is a calculated vibrational frequency at 1375 cm^{-1} which has strong Raman activity and is associated with the N═N bond stretching and N−H bond bending vibration modes (see Figure 7 and Table 1S ν_{93} in the Supporting Information), but in the TR^3 spectrum, the band intensity at 1374 cm^{-1} is very small. Besides the reason mentioned above that the experimental spectrum is resonantly enhanced whereas the calculated spectrum is for normal (or nonresonance) Raman spectra, this may also be due to the effect of the real superwater molecule system. The presence of a water molecule and hydroxide ion affects the existence of the form of the azo cation. The interaction between the *cis* azo cation and the hydroxide ion elongates the N═N in *cis* azo cation and consequently decreases in a distinct manner the Raman activity associated the N═N stretching. This has been found in the DFT calculations for the *cis* azo cation. Figure 7 displays B3LYP/6-31g* calculated normal Raman spectra for the *cis* azo cation with and without a hydroxide ion around it. This comparison clearly shows that with the hydroxide ion nearby, the Raman activity of the N═N stretching mode indicated with a star symbol decreases. Moreover, there are very complicated interactions such as hydrogen bonding that will exist between the water molecules and the reactants and also the intermediate molecules. All of these effects and interactions exist under real experimental conditions, but they are difficult to effectively mimic by using our basic theoretical calculations here.

Discussion of the 4-Biphenylnitrenium ion Reaction with 4-Biphenyl Azide. The 4-biphenylnitrenium ion can react with its unphotolyzed precursor, 4-biphenyl azide to produce a 4,4′-azobisbiphenyl cation intermediate first and then lose H^+ to give rise to a stable 4,4′-azobisbiphenyl product. To our knowledge,

TABLE 3: Dihedral Angles between the Two Close Aromatic Rings in the 4-Biphenyl Species

dihedral angel	*cis* complex	TS1	PC1	TS3	PC3a	TS4	PC3b	*cis*-azo	*trans* complex	TS2	PC2	*trans*-azo
A−B	31.64	34.69	34.43	35.36	28.45	35.65	35.49	37.50	32.63	35.61	29.59	36.87
C−D	24.48	33.55	35.46	36.89	32.24	37.21	37.84	37.55	23.27	29.54	32.00	36.87

this is the first time that the cation intermediate in this kind of reaction is directly observed by using time-resolved vibrational spectroscopy. Previously, we studied the reaction of the 2-fluorenylnitrenium ion with 2-fluorenyl azide to produce 2,2′-azobisfluorene[25] and observed that the 2,2′-azobisfluorene formation and the 2-fluorenylnitrenium ion decay can be fitted by a common time constant, and no intermediates between the nitrenium ion and the azo compound was seen. This difference is mainly due to the rigid structure of two aromatic rings in the 2-fluorenyl species and the more flexible rotatable structure of those in the 4-biphenyl species. The rotation of the aromatic rings in the 4-biphenyl species significantly stabilizes the geometries as shown in Table 3, which lists the dihedral angles between the two close aromatic rings. As the reaction goes from the reactant complex through the transition states to the intermediates, the dihedral angles between the two close aromatic rings change distinctly by about 10°. In addition, the flexibility of the bond connecting the two phenyl rings leads the 4-biphenylnitrenium ion to have a smaller iminocyclohexadienyl character compared to the rigid planar structure of the 2-fluorenylnitrenium ion.[22]

Previous transient absorption quenching experiments determined that the 4-biphenylnitrenium ion reacts with the azide anion (N_3^-) and water molecules with rate constants in the diffusion limit and 2×10^6 s^{-1}, respectively.[35] The 4-biphenylnitrenium ion was also observed to react with deoxyguanosine with a rate constant of 2×10^9 M^{-1} s^{-1}.[35] Here, our results indicates that the 4-biphenylnitrenium ion can react with 4-biphenyl azide with a rate constant on the order of 2.7×10^9 M^{-1} s^{-1} and quenching of the 4-biphenylnitrenium ion occurs predominantly by reaction with the remaining 4-biphenyl azide at the concentrations examined here. The rate constant for reaction of the 4-biphenylnitrenium ion with 4-biphenyl azide is substantially faster than that for the 4-biphenylnitrenium ion with water (2×10^6 s^{-1}) and is comparable to the 4-biphenylnitrenium ion with guanosine (about 2×10^9 M^{-1} s^{-1}) to form a C8 intermediate species. Thus, guanosine or other guanine derivatives can compete with quenching of the 4-biphenylnitrenium ion by the parent 4-biphenyl azide species when the guanosine (or other guanine derivatives) have concentrations similar to or greater than the concentration of the remaining unphotolyzed 4-biphenylazide.

When the 4-biphenylnitrenium ion is quenched by N_3^- or water, the target in the nitrenium ion is an *ortho* or *para* aromatic carbon atom. But the reactive position is the nitrogen of the nitrenium ion when the nitrenium ion reacts with the guanine derivatives. At this point, the reaction of the 4-biphenylnitrenium ion with 4-biphenyl azide is similar to the reaction of the 4-biphenylnitrenium ion toward guanine derivatives. The dipolar structures of aryl azides (Figure 8) proposed by Pauling[36] can

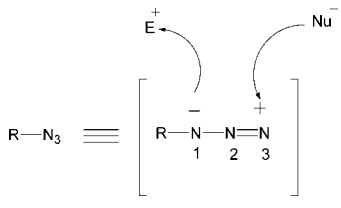

Figure 8. Reactivity of aryl azides.[37]

explain the azides chemical reactivity. In principle, they react with electrophiles at N^1 and nucleophiles at N^3. As in the case of the nitrene chemistry, it was suggested that the arylnitrene (ArN) reacts at N^1 of the azide (ArN_3) to make the azo product (reaction 1). It was also suggested that the azide group protonation by a Lewis acid at N^1 leads to a migration of another phenyl substituent with the loss of nitrogen gas[38] (reaction 2).

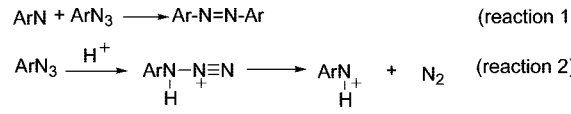

Reactions 1 and 2 are similar in that both appear to add to the N^1 of the azide to form the corresponding azo product with the elimination of a nitrogen gas byproduct. Our present results indicate that the 4-biphenylnitrenium ion undergoes similar addition reactions which form a stable azo product (4,4′-azobisbiphenyl) with elimination of a nitrogen gas byproduct. The observation of an azo cation clearly demonstrates that the reaction of the 4-biphenylnitrenium ion + 4-biphenyl azide → 4,4′-azobisphenyl + N_2 + H^+ is a sequential process.

Conclusion

The reaction of the 4-biphenylnitrenium ion with 4-biphenyl azide in a mixed aqueous solution produces 4,4′-azobisbiphenyl through an intermediate species. With the help of DFT calculations, the intermediate was tentatively assigned to a 4,4′-azobisbiphenyl cation-type intermediate. The direct observation of the 4,4′-azobisbiphenyl cation intermediate demonstrates that the reaction of the 4-biphenylnitrenium ion with 4-biphenyl azide produces the 4,4′-azobisbiphenyl with nitrogen gas and hydrogen cation byproducts in a sequential process. DFT calculations predict that the reaction of the 4-biphenylnitrenium ion with 4-biphenyl azide can proceed on two parallel and competing pathways to produce *cis* and *trans* azo products. On the *cis* pathway, the new bond formation between nitrogen of the nitrenium ion and N^1 of the azide and the elimination of nitrogen gas take place in a stepwise manner, but on the *trans* pathway, these two processes appear to be concerted.

Experiment and Computation Methods

Samples of 4-biphenyl azide and 4,4′-azobisbiphenyl were synthesized according to the literature methods,[1,33] and further details of the synthesis and characterization are given in ref 29. The 4-biphenyl azide samples were prepared with concentrations ~1 and ~2 mM in water:acetonitrile (60:40 by volume) solvent for use in the TR^3 experiments. Spectroscopic grade acetonitrile and distilled water were used in preparing the sample solutions.

The experimental apparatus and methods used to obtain the nanosecond time-resolved resonance Raman (ns-TR^3) experiments have been detailed previously;[19,21,22,24] therefore, only a short description is presented in this section. The hydrogen Raman shifted laser lines for the harmonics of a Nd:YAG nanosecond pulsed laser system produced the 299.1 nm pump (e.g., the first Stokes Raman shifted line of the 266 nm fourth harmonic of the Nd:YAG laser) and 354.7 nm probe (the third harmonic of the Nd:YAG laser) wavelengths employed in the

ns-TR^3 experiments. The ns-TR^3 experiments utilized two Nd:YAG lasers electronically synchronized to each other by a pulse delay generator used to control the relative timing of the two lasers (with a jitter <5 ns) that was monitored by using a fast photodiode and a 500 MHz oscilloscope. The pump and probe laser beams were lightly focused onto a flowing liquid stream of sample by using a near collinear backscattering geometry, and the Raman scattered light was collected by using a backscattering geometry and reflective optics that imaged the light through a depolarizer and entrance slit of a 0.5 m spectrograph that dispersed the light onto a liquid-nitrogen-cooled CCD detector. The Raman signal was acquired for about 30−60 s before being read out to an interfaced PC computer and about 10−20 of these read outs were summed to obtain the Raman spectrum. The TR^3 spectra were determined by subtracting the pump−probe spectrum at negative 100 ns from the pump−probe spectra acquired at positive delay times so as to remove the solvent and precursor Raman bands, and the known wavenumbers of the mixed solvent acetonitrile Raman bands were used to calibrate the wavenumber of the TR^3 spectra to an absolute accuracy of about ± 3 cm^{-1} (and a relative accuracy of $\pm 1-2$ cm^{-1} from scan to scan). A Lorentzian function was utilized to integrate the relevant Raman bands to find their areas and determine the decay and growth kinetics of the species observed in the TR^3 experiments.

All of the DFT calculations made use of the Gaussian 98 program suite.[34] The complete geometry optimizations were carried out analytically by using the (U)B3LYP method with the 6-31g* basis set for the species of interest. Vibrational frequency calculations were performed for all of the stationary points to obtain correction for the zero-point energies and to ascertain that the computed transition states were the first-order saddle points. IRC computations were done to confirm that the transition states connected the appropriate reactants and products. The solvent effect on the reaction was examined here by employing B3LYP/6-31g* optimizations of the gas-phase stationary points and by using a relatively simple self-consistent reaction field (SCRF)[30] method based on the polarizable continuum model (PCM).[31] A Lorentzian function with a 20 cm^{-1} bandwidth was used in conjunction with the calculated Raman vibrational frequencies and relative intensities to find the calculated B3LYP/6-31g* Raman spectra presented here.

Acknowledgment. This work was supported by grants from the Research Grants Council (RGC) of Hong Kong (HKU 7040/06P) to D.L.P. D.L.P. thanks the Croucher Foundation for the award of a Croucher Foundation Senior Research Fellowship (2006-07) and the University of Hong Kong for an Outstanding Researcher Award (2006).

Supporting Information Available: Figure 1S. Overview of the 354.7 nm probe wavelength TR^3 spectra obtained after 299.1 nm photolysis of 2 mM 4-biphenyl azide in a water:acetonitrile(60:40 by volume) mixed solvent. Figure 2S. Comparison of the 10 ns TR^3 spectra from Figure 1 with 354.7 nm as the probe wavelength to that obtained with 416.0 nm as the probe wavelength reported previously in reference.[22] Figure 3S. Comparison of the B3LYP/6-31g* calculated normal Raman spectrum for *trans* 4,4′-azobisbiphenyl to the experimental 100 μs TR^3 spectrum from Figure 1S and the 354.7 nm resonance Raman spectrum of synthesized 4,4′-azobisbiphenyl. Figure 4S. Absorption spectra of 4-biphenyl azide and synthesized 4,4′-azobisbiphenyl. Figure 5S. Comparison of the intermediate observed in Figures 1 and 1S to the 354.7 nm probe TR^3 spectrum of the triplet 4-biphenylnitrene species obtained at 10 ns after photolysis of 2 mM 4-biphenyl azide in neat acetonitrile. Table 1S. Comparison of the experimental TR^3 vibrational frequencies for the intermediate to those obtained from B3LYP/6-31g* calculations for the *trans* azo cation. Table 2S. Comparison of the experimental TR^3 vibrational frequencies for the intermediate to those obtained from the B3LYP/6-31g* calculations for the *cis* azo cation. Cartesian coordinates, total energies, and vibrational zero-point energies for the optimized geometry from the B3LYP/6-31g* calculations for the structures calculated in this paper. This material is available free of charge via the Internet at http://pubs.acs.org.

References and Notes

(1) Wheeler, O. H.; Gonzalez, D. *Tetrahedron* **1964**, *20*, 189–193.
(2) Scribner, J. D.; Miller, J. A.; Miller, E. C. *Cancer Res.* **1970**, *30*, 1570–1579.
(3) Scribner, J. D.; Naimy, N. K. *Cancer Res.* **1975**, *35*, 1416–1421.
(4) Miller, E. C. *Cancer Res.* **1978**, *38*, 1479–1496.
(5) Miller, E. C.; Miller, J. A. *Cancer* **1981**, *47*, 2327–2345.
(6) Singer, B.; Kusmierek, J. T. *Annu. Rev. Biochem.* **1982**, *51*, 655–691.
(7) Miller, J. A.; Miller, E. C. *Environ. Health Perspect.* **1983**, *49*, 3–12.
(8) Famulok, M.; Boche, G. *Angew. Chem., Int. Ed. Engl.* **1989**, *28*, 468–469.
(9) Meier, C.; Boche, G. *Tetrahedron Lett.* **1990**, *31*, 1693–1696.
(10) Humphreys, W. G.; Kadlubar, F. F.; Guengerich, F. P. *Proc. Natl. Acad. Sci. U. S. A.* **1992**, *89*, 8278–8282.
(11) Novak, M.; Kennedy, S. A. *J. Am. Chem. Soc.* **1995**, *117*, 574–575.
(12) Kennedy, S. A.; Novak, M.; Kolb, B. A. *J. Am. Chem. Soc.* **1997**, *119*, 7654–7664.
(13) McClelland, R. A.; Ahmad, A. R.; Dicks, A. P.; Licence, V. E. *J. Am. Chem. Soc.* **1999**, *121*, 3303–3310.
(14) Cheng, B.; McClelland, R. A *Can. J. Chem.* **2001**, *79*, 1881–1886.
(15) Davidse, P. A.; Kahley, M. J.; McClelland, R. A.; Novak, M. *J. Am. Chem. Soc.* **1994**, *116*, 4513–4514.
(16) Srivastava, S.; Toscano, J. P.; Moran, R. J.; Falvey, D. E. *J. Am. Chem. Soc.* **1997**, *119*, 11552–11553.
(17) Srivastava, S.; Ruane, P. H.; Toscano, J. P.; Sullivan, M. B.; Cramer, C. J.; Chiapperino, D. C.; Reed, E. C.; Falvey, D. E. *J. Am. Chem. Soc.* **2000**, *122*, 8271–8278.
(18) McClelland, R. A.; Davidse, P. A.; Hadzialic, G. *J. Am. Chem. Soc.* **1995**, *117*, 4173–4174.
(19) Chan, P. Y.; Ong, S. Y.; Zhu, P.; Zhao, C.; Phillips, D. L. *J. Phys. Chem. A.* **2003**, *107*, 8067–8074.
(20) McClelland, R. A.; Kahley, M. J.; Davidse, P. A. *J. Phys. Org. Chem.* **1996**, *9*, 355–360.
(21) Zhu, P.; Ong, S. Y.; Chan, P. Y.; Leung, K. H.; Phillips, D. L. *J. Am. Chem. Soc.* **2001**, *123*, 2645–2649.
(22) Zhu, P.; Ong, S. Y.; Chan, P. Y.; Poon, Y. F.; Leung, K. H.; Phillips, D. L. *Chem. Eur. J.* **2001**, *7*, 4928–4936.
(23) Kwok, W. M.; Chan, P. Y.; Phillips, D. L. *J. Phys. Chem. B* **2004**, *108*, 19068–19075.
(24) (a) Chan, P. Y.; Kwok, W. M.; Lam, S. K.; Chiu, P.; Phillips, D. L. *J. Am. Chem. Soc.* **2005**, *127*, 8246–8247. (b) Xue, J.; Chan, P. Y.; Du, Y.; Guo, Z.; Chung, C. W. Y.; Toy, P. H.; Phillips, D. L. *J. Phys. Chem. B* **2007**, *111*, 12676–12684.
(25) Xue, J.; Guo, Z; Chan, P. Y.; Chu, L. M.; But, T. Y. S.; Phillips, D. L. *J. Phys. Chem. A.* **2007**, *111*, 1441–1451.
(26) Wang, J.; Burdzinski, G.; Zhu, Z.; Platz, M. S.; Carra, C.; Bally, T. *J. Am. Chem. Soc.* **2007**, *129*, 8380–8388.
(27) McClelland, R. A.; Kahley, M. J.; Davidse, P. A.; Hadzialic, G. *J. Am. Chem. Soc.* **1996**, *118*, 4794–4803.
(28) Tsao, M.-L.; Gritsan, N.; James, T. R.; Platz, M. S.; Hrovat, D. A.; Borden, W. T. *J. Am. Chem. Soc.* **2003**, *125*, 9343–9358.
(29) Chan, P. Y.; Ong, S. Y.; But, T. Y. S.; Phillips, D. L. *J. Raman. Spectrosc.* **2004**, *35*, 887–894.
(30) (a) Tapia, O. *J. Math. Chem.* **1992**, *10*, 139–181. (b) Tomasi, J.; Persico, M. *Chem. Rev.* **1994**, *94*, 2027–2094. (c) Simkin, B. Y.; Sheikhet, I. *Quantum Chemical and Statistical Theory of solutions- A computational approach*; Ellis Horwood: London, 1995.
(31) (a) Cances, E.; Mennucci, B.; Tomasi, J. *J. Chem. Phys.* **1997**, *107*, 3032–3041. (b) Cossi, M.; Barone, V.; Cammi, R.; Tomasi, J. *Chem. Phys. Lett.* **1996**, *255*, 327–335. (c) Barone, V.; Cossi, M.; Tomasi, J. *J. Comput. Chem.* **1998**, *19*, 404–417.
(32) Nagele, T.; Hoche, R.; Zinth, W.; Wachtveitl, J. *Chem. Phys. Lett.* **1997**, *272*, 489–495.

(33) Brown, B. R.; Yielding, L. W.; White, W. E *Mutat. Res.* **1980**, *70*, 17–27.

(34) Frisch, M. J.; Trucks, G. W.; Schlegel, H. B.; Scuseria, G. E.; Robb, M. A.; Cheeseman, J. R.; Zakrzewski, V. G.; Montgomery, J. A., Jr.; Stratmann, R. E.; Burant, J. C.; Dapprich, S.; Millam, J. M.; Daniels, A. D.; Kudin, K. N.; Strain, M. C.; Farkas, O.; Tomasi, J.; Barone, V.; Cossi, M.; Cammi, R.; Mennucci, B.; Pomelli, C.; Adamo, C.; Clifford, S.; Ochterski, J.; Petersson, G. A.; Ayala, P. Y.; Cui, Q.; Morokuma, K.; Malick, D. K.; Rabuck, A. D.; Raghavachari, K.; Foresman, J. B.; Cioslowski, J.; Ortiz, J. V.; Stefanov, B. B.; Liu, G.; Liashenko, A.; Piskorz, P.; Komaromi, I.; Gomperts, R.; Martin, R. L.; Fox, D. J.; Keith, T.; Al-Laham, M. A.; Peng, C. Y.; Nanayakkara, A.; Gonzalez, C.; Challacombe, M.; Gill, P. M. W.; Johnson, B. G.; Chen, W.; Wong, M. W.; Andres, J. L.; Head-Gordon, M.; Replogle, E. S.; Pople, J. A. *Gaussian 98*, revision B.05; Gaussian, Inc.: Pittsburgh, PA, 1998.

(35) McClelland, R. A.; Gadosy, T. A.; Ren, D. *Can, J. Chem* **1998**, *76*, 1327–1337.

(36) (a) Pauling, L.; Brockway, L. O. *J. Am. Chem. Soc.* **1937**, *59*, 13–20. (b) Brockway, L. O.; Pauling, L. *Natl. Acad. Sci. U. S. A.* **1933**, *19*, 860–867.

(37) Brase, S.; Gil, C.; Knepper, K.; Zimmermann, V. *Angew. Chem., Int. Ed.* **2005**, *44*, 5188–5240.

(38) Desai, P.; Schildknegt, K.; Agrios, K. A.; Mossman, C.; Milligan, G. L.; Aube, J. *J. Am. Chem. Soc.* **2000**, *122*, 7226–7232.

JP805353Q